

Thermo-elastic response of the Juno spacecraft's solar array/magnetometer boom

Matija Herceg¹, Peter S Jorgensen¹, John L Jorgensen², and John E. P. Connerney³

¹Technical University of Denmark

²DTU Space, National Space Institute, Technical University of Denmark

³NASA Goddard Space Flight Center

November 25, 2022

Abstract

Juno was inserted into a highly elliptic, polar, orbit about Jupiter on July 4th 2016. Juno's magnetic field investigation acquires vector measurements of the Jovian magnetic field using a flux gate magnetometer co-located with attitude-sensing star cameras on an optical bench. The optical bench is placed on a boom at the outer extremity of one of Juno's three solar arrays. The Magnetic Field investigation (MAG) uses measurements of the optical bench inertial attitude provided by the micro Advanced Stellar Compass (μ ASC) to render accurate vector measurements of the planetary magnetic field. During periJoves, MAG orientation is determined using the spacecraft (SC) attitude combined with transformations between SC and MAG. Substantial pre-launch efforts were expended to maximize the thermal and mechanical stability of the Juno solar arrays and MAG boom. Nevertheless, flight experience demonstrated that the transformation between SC and MAG reference frames varied significantly in response to spacecraft thermal excursions associated with large attitude maneuvers and proximate encounters with Jupiter. This response is monitored by comparing attitudes provided by the MAG investigation's four CHU's and the spacecraft attitude. These attitude disturbances are caused by the thermo-elastic flexure of the Juno solar array in response to temperature excursions associated with maneuvers and heating during close passages of Jupiter. In this paper, we investigate these thermal effects and propose a model for compensation of the MAG boom flexure effect.

34 **1 Introduction**

35 As a fully autonomous star tracker, the MAG's micro Advanced Stellar Compass (μ ASC)
36 services the Juno MAG attitude determination requirement by comparison of the star field with a
37 matching star field stored in an on-board star catalog (Connerney et al., 2017). Juno's MAG
38 boom is a four-meter extension at the outer extremity of one of Juno's three solar panel arrays.
39 Juno is a spin-stabilized spacecraft rotating nominally at 2 rotations per minute (rpm) about the z
40 axis which is closely aligned with the spacecraft telecommunications antenna. To optimize the
41 attitude determination function on a spinning spacecraft, the four μ ASC star cameras (CHUs) are
42 oriented on the Juno spacecraft with an angular separation of 13° between optical and spin axes.
43 The CHUs have an optical field of view (FOV) of 13° by 18° and scan the sky continuously in
44 the anti-sunward direction, imaging every 0.25 seconds and producing attitude quaternions at
45 that rate (though telemetry allocations dictate downlink cadence).

46 The MAG investigation was planned with several pathways to provide attitude determination for
47 the fluxgate sensors (Connerney et al., 2017), and that flexibility proved useful when Juno's
48 mission plan transitioned, after orbit insertion, from one with 14-day orbits to one with 53-day
49 orbits (Bolton et al., 2017). To acquire the same number (34) of orbits provided for in the
50 original mission plan, Juno would be required to operate over a much broader range of local
51 times than it was designed for. As a result, during most periJoves, the ASC CHUs would
52 encounter Jupiter in the FOV for at least some of the time, preventing continuous attitude
53 determination throughout the critical periJove passage. As a result, the MAG investigation
54 elected a backup attitude determination strategy in which attitudes are derived from the
55 spacecraft attitude solution (c-kernel) using a transformation between the MAG optical bench
56 and the spacecraft determined by comparison (when available) between the ASC CHUs and the
57 spacecraft SRU.

58 Direct comparison of the spacecraft attitude solutions with those provided by the CHUs on the
59 MAG boom revealed a systematic variation in the attitude of the MAG Boom as Juno transited
60 the solar system during cruise, attributed to mechanical deformation of the solar array as it
61 cooled while moving further from the sun (Connerney et al., 2017). Once Juno arrived on orbit, a
62 similar deformation was observed during periJove passes, attributed to heating of the solar array
63 by Jupiter. We note that the MAG boom itself proved to be remarkably stable, throughout cruise
64 and during orbital operations, but as it is affixed to the outer end of the solar array, a distortion of
65 the array perturbs the attitude of the MAG Boom. The solar array bends in response to the
66 increase in temperature due to non-isotropic coefficient of thermal expansion (CTE) related to
67 the design of the mechanical assemblage. The array substrate can be thought of as a sandwich
68 consisting of thin carbon-composite face sheets encasing an aluminum honeycomb core (typical
69 of lightweight spacecraft construction). By itself it would likely be fairly benign in its thermal

70 response, but one side (sunward facing) is coated with silicon cells and cover glass, with a CTE
71 unlike that of the substrate.

72 The increase in temperature associated with a periJove passage is measured by multiple thermal
73 sensors on the solar array and is just a few degrees C (about 5 or 6 degrees for most periJoves)
74 from a typical baseline temperature of about -130° C. However, that is sufficient to alter the
75 boom (and MAG sensor) attitude by almost 0.1° . This thermal distortion is brief in duration (~ 2
76 hours) and the array returns to its pre-periJove attitude after thermal relaxation, but the distortion
77 occurs at the time of highest scientific interest. An attitude determination error of this magnitude
78 would compromise the vector accuracy of the magnetic field measurement (in strong magnetic
79 fields) if not corrected for. Since Juno periapsis passages are just above the planet's cloudtops,
80 and Jupiter has a very strong planetary magnetic field (Connerney et al., 2018), every passage
81 transits a strong magnetic field magnitude (~ 4 to ~ 16 G).

82 Identification of the thermal distortion of the solar array necessitated implementation of a time
83 dependent transformation between spacecraft and MOB. The objective of this study is to
84 characterize the thermal distortion of the mechanical appendage, determine its dependence on
85 array temperature, and offer a model whereby the attitude disturbance can be predicted with
86 confidence and removed from the data. This report also serves to bring awareness to subtle
87 effects that may limit measurement accuracy on flight systems that do not benefit from sensors
88 capable of monitoring mechanical stability.

89

90 2 Modeling of the thermo-elastic effects

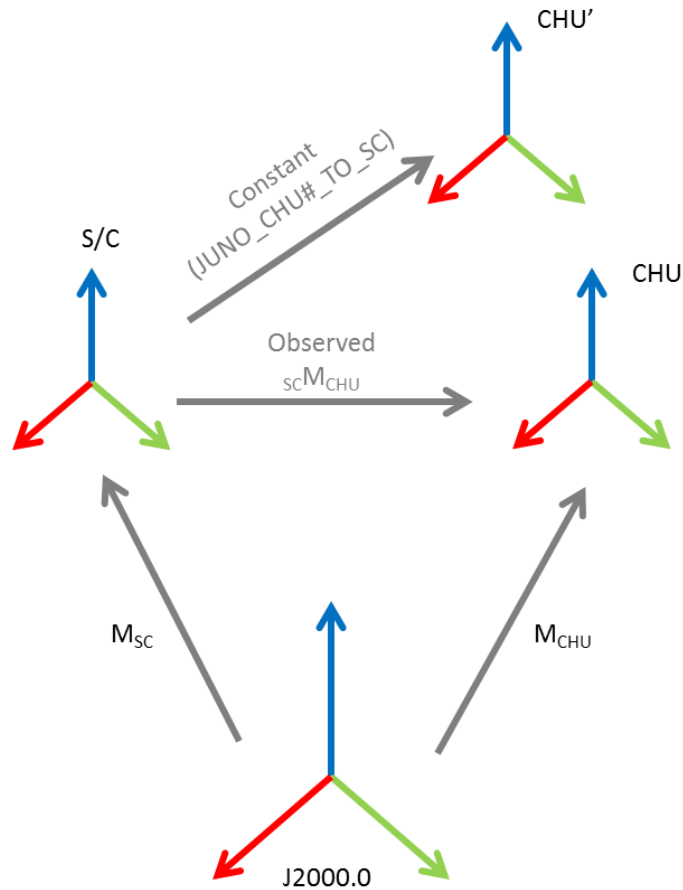
91 The relevant Juno reference frames, and the transformations between them, are presented in Fig
92 1. M_{SC} is the transformation matrix describing the Juno spacecraft orientation in the inertial
93 (J2000) reference frame, extracted from NAIF c-krenels, and M_{CHU} is the transformation matrix
94 describing the orientation of a CHU in the inertial (J2000) frame, determined from μ ASC
95 measurements. Fixed transformations between the Juno SC and each of the 4 ASC CHU's
96 ($Juno_CHU\#_TO_SC$), as defined in the NAIF frame (FK) kernel file, may be represented via
97 sequential rotations about the spacecraft x, y, and z axes (Table 1).

98

	Rot3 Z	Rot3 Y	Rot3 X
S/C->CHU A	178.950	1.370	-167.035
S/C->CHU B	179.125	1.150	167.035
S/C->CHU C	-1.000	0.480	-166.480
S/C->CHU D	-0.220	0.510	167.380

99 **Table 1: Fixed transformations between the Juno SC and each of the 4 ASC CHU's,**
100 **represented via sequential rotations about the spacecraft x, y, and z axes**

101



102

103 **Figure 1: Coordinate frames utilized for the thermo-elastic boom model and relations**
 104 **between them.**

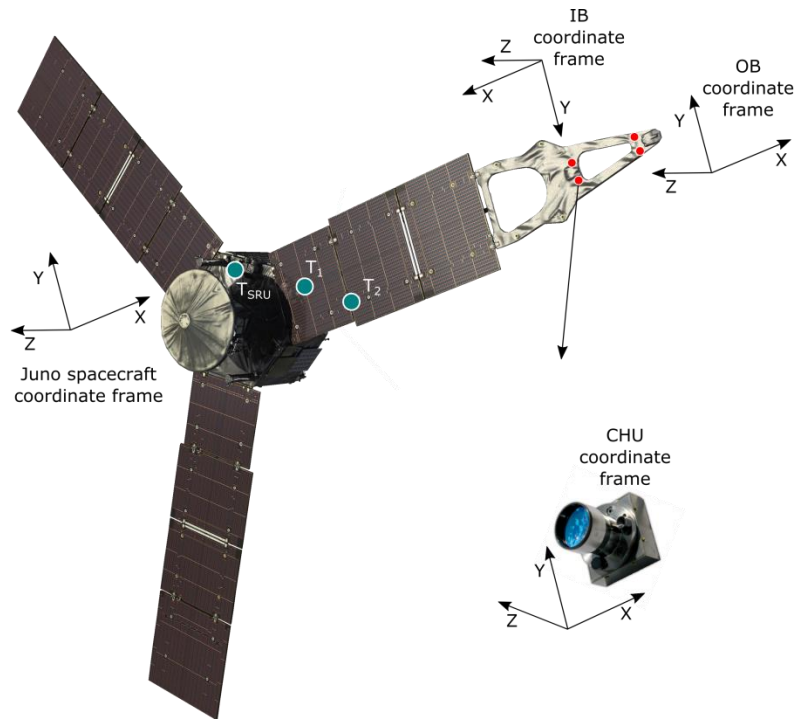
105

106 The transformation from the SC frame to that of the InBoard (IB) or OutBoard (OB) MOBs (see
 107 Fig 2) was originally envisioned as a static transformation that might change from one periJove
 108 to another, perhaps in response to infrequent spacecraft propulsive maneuvers, but was assumed
 109 to remain unchanged throughout a periJove pass. The MAG boom itself proved to be remarkably
 110 stable over environmental conditions, as determined by inter-comparison of the four CHUs. Each
 111 MOB contains a pair of CHUs, mounted to the MOB with kinematic mounts (as are the fluxgate
 112 sensors) which have proven remarkably stable. The MAG boom itself is a large (~4m) 3-
 113 dimensional structure constructed of aluminum honeycomb, carbon-composite faced, with
 114 longitudinal stiffeners running the length of the structure, fully enclosed in multi-layer thermal
 115 insulating blankets.

116 The MAG investigation anticipated the need to verify in flight the deployment attitude of the
 117 MAG boom, and periodically monitor the relationship between spacecraft attitude and MOB
 118 attitude, and as a result a series of attitude calibration exercises were scheduled before and after

119 major propulsive maneuvers (Connerney et al., 2017). We learned that while propulsive
 120 maneuvers resulted in transient disturbances, the MAG boom attitude returned very close to pre-
 121 maneuver orientation. However, when comparing the spacecraft attitude solution during periJove
 122 passages with attitudes measured each 0.24 s by the CHUs, we observed a systematic variation
 123 quickly identified as a response of the Juno solar array to the increase in temperature due to
 124 Jupiter thermal emission. Thus the need for a predictive model resulting in a time-dependent
 125 transformation between spacecraft and MOB.

126



127

128 **Figure 2: The Juno spacecraft, the μ ASC CHU and the MAG instrument coordinate**
 129 **frames. Turquoise circles show locations of the Wing 1 solar array thermistors (T_1 and T_2)**
 130 **and Stellar Reference Unit thermistors (T_{SRU}). Red circles show locations of the four μ ASC**
 131 **CHU's. Rotation about the y-axis of the SC is where bending of the Juno wing 1 is**
 132 **observed.**

133

134

135 Comparison of the CHU attitude observations and SC orientation in the CHU reference frame
 136 (${}_{sc}M_{chu}$) shows a systematic variation with periJove passage, remarkably consistent from one
 137 periJove passage to the next (Fig 3) with one exception having to do with spacecraft attitude
 138 during periJove passage. Most orbits in the Juno mission plan are executed with the spacecraft

139 spin axis, and telecom antenna, directed toward Earth for gravity science (Bolton et al., 2017).
 140 On occasion, periJoves are executed with the spin axis directed off Earth-point in a manner that
 141 optimizes passage of the microwave radiometer (MWR) field of view (and that of other
 142 instruments) as it scans across the planet. These two kinds of orbits – called ‘GRAV’ and
 143 ‘MWR’ orbits for short – lead to different thermal responses most easily identified by the
 144 attitude of the Mag boom upon approach to periJove and the disturbance in attitude ~6 hours
 145 after periJove as the spacecraft re-acquires Earth pointed attitude.

146 Transformation between the SC and CHU frame is (${}_{sc}M_{chu}$) is defined as:

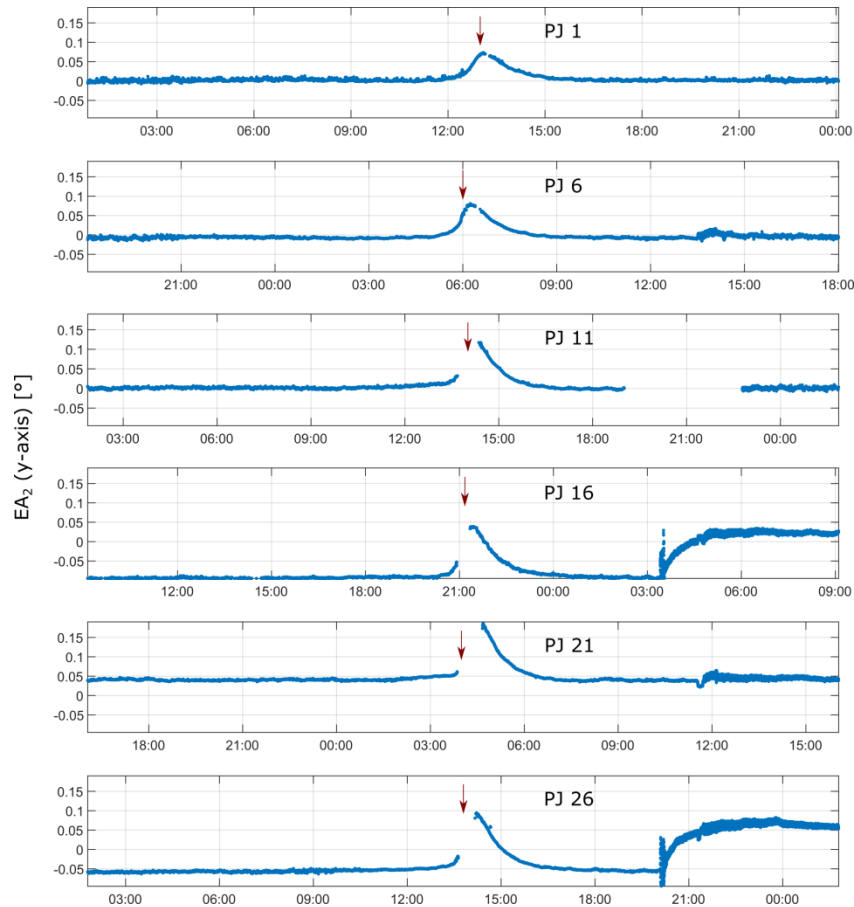
147
$${}_{sc}M_{chu} = M_{CHU} \cdot M_{SC}^T \tag{1}$$

148 Comparison of the Juno CHU and SC orientation in the CHU reference frame is calculated by
 149 applying the preflight fixed transformations between the two frames:

150
$${}_{sc}M_{chu_REL} = M_{Juno_CHU\#_TO_SC} \cdot {}_{sc}M_{chu}^T \tag{2}$$

151

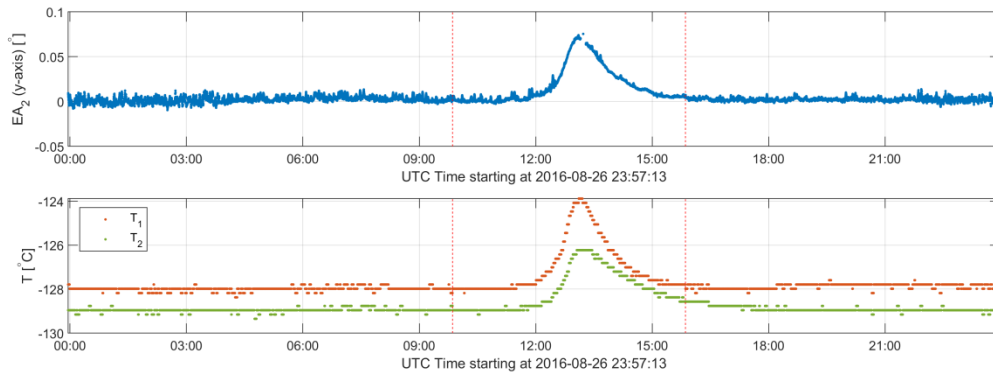
152



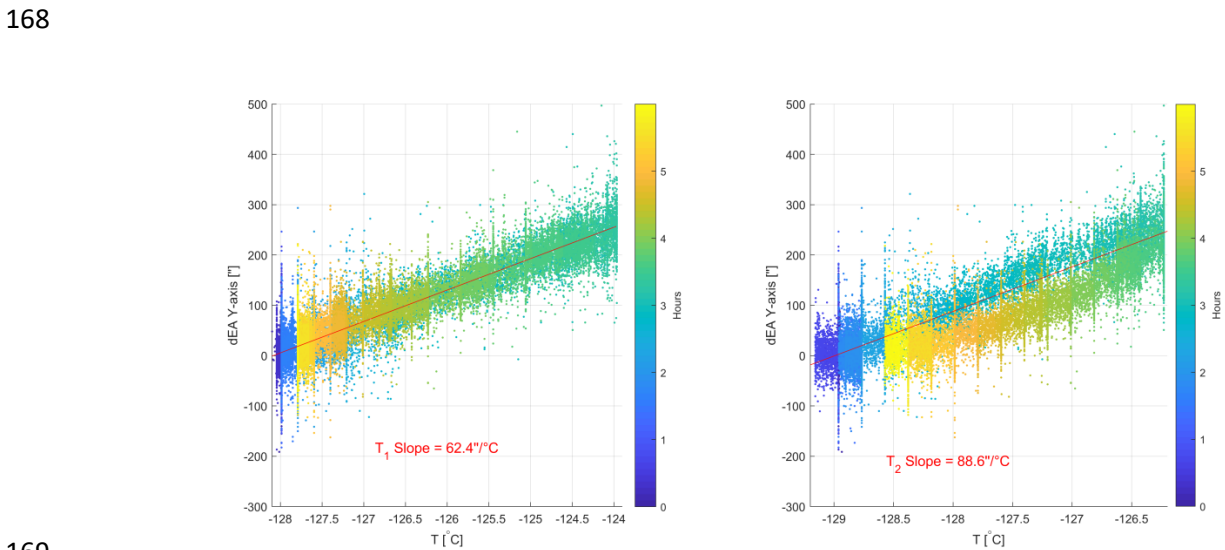
153

154 **Figure 3: Comparison of the Juno CHU B and SC orientation expressed as a rotation about**
 155 **the spacecraft y-axis in the CHU reference frame (for the PJ 1, 6, 11, 16, 21 and 26). A fixed**
 156 **rotation (bias) about y-axis of 1.15° has been removed. PJs 16 and 26 illustrate MWR**
 157 **orbits, in which the spacecraft approaches Jupiter off Earth-point, and returns to Earth**
 158 **pointed attitude ~6 hours post-PJ. Red arrows indicate the time of the periJove.**

159 The Juno spacecraft is equipped with a multitude of thermal sensors to monitor temperatures
 160 throughout the spacecraft, including several deployed along the solar array (wing #1) hosting the
 161 MAG boom. Two of these (T1 and T2 in Figure 2) have proven very useful in modeling the
 162 array response, as illustrated in Figure 4. Comparison of the temperature and attitude variation
 163 shows a clear correlation between the disturbance rotation angle about the CHU B y-axis and the
 164 solar array temperature (bottom two panels, Figure 4).



165
 166 **Figure 4: Juno SC rotation about the y-axis in the CHU B reference frame for PJ 1 (top**
 167 **plot), Juno wing 1 solar panel thermistor observations (T₁ and T₂, second plot)**



170 **Figure 5: Correlation between the rotation about the y-axis variation and Juno solar panel**
 171 **temperatures (T_1 and T_2). Correlation is shown for the period +/- 3 hours around the**
 172 **periJove**

173

174 For the purpose of correcting the relative orientation between the SC and each CHU for thermal
 175 effects, a thermal compensation model was defined using valid attitude data from the very first
 176 periJove (PJ 1). A model was constructed using the orientation of each CHU with respect to the
 177 SC orientation in the camera frame combined with Juno wing 1 solar panel temperatures T_1 and
 178 T_2 . T_1 is a compact reference for Lockheed Martin’s (LM) engineering telemetry channel T-0237
 179 SA1pan1Temp, and T_2 refers to LM’s T-0446 SA1pan2Temp, output from Juno’s wing 1 solar
 180 panel thermistors. In addition to the solar panel temperatures, T_1 and T_2 , the model uses Stellar
 181 Reference Unit (SRU) thermistors to compensate for the small quasi-periodic attitude
 182 perturbations visible on the x-axis. These relatively minor attitude errors (in the spacecraft c-
 183 kernel attitude estimation) are caused by the slight thermal distortion of the mechanical structure
 184 supporting the SRU. These perturbations correlate well with a combination of the outputs from
 185 the two thermistors associated with this subsystem; the SRU is heated by two independently-
 186 controlled heaters cycling on and off in a quasi-periodic manner. We use the SRU-based
 187 temperature proxy T_{SRU} that is the mean of the SRU temperatures
 188 ($T_{SRU}=(SRU1_{Temp1}+SRU2_{Temp1})/2$).

189 To estimate the parameters of the thermal model (rotations) based on the observed temperatures
 190 and frames differences, a Singular Value Decomposition (SVD) of the linear system of equations
 191 was used. The resulting thermal model describes how each transformation between CHU and SC
 192 changes due to the observed temperature of the Juno wing 1 structure and it is defined as:

$$193 \quad M_{Juno_CHU\#_TO_SC_CORR} = R_1(\alpha) \cdot R_2(\beta) \cdot R_1(\gamma) \cdot M_{Juno_CHU\#_TO_SC} \quad (3)$$

194

195 Where each rotation is described by:

$$196 \quad R_1(\alpha) = \begin{bmatrix} 1 & 0 & 0 \\ 0 & \cos(\alpha) & \sin(\alpha) \\ 0 & -\sin(\alpha) & \cos(\alpha) \end{bmatrix} \quad (4)$$

197

$$198 \quad R_2(\beta) = \begin{bmatrix} \cos(\beta) & 0 & -\sin(\beta) \\ 0 & 1 & 0 \\ \sin(\beta) & 0 & \cos(\beta) \end{bmatrix} \quad (5)$$

199

200

$$R_3(\gamma) = \begin{bmatrix} \cos(\gamma) & \sin(\gamma) & 0 \\ -\sin(\gamma) & \cos(\gamma) & 0 \\ 0 & 0 & 1 \end{bmatrix} \quad (6)$$

201

202 And individual rotation angles are represented as follows:

$$\alpha = \alpha_0 + \alpha_1 T_1 + \alpha_2 T_2 + \alpha_3 T_{SRU} \quad (7)$$

$$\beta = \beta_0 + \beta_1 T_1 + \beta_2 T_2 + \beta_3 T_{SRU} \quad (8)$$

205

206 Model derived from the SVD is shown in Table 1.

207 Resulting thermal model coefficients derived from SVD is shown in *Table 2*.

208

CHU A				
	α	β	γ	
Constant	0.0836	-2.3869	-0.3924	[°]
T₁	0.0019	-0.0140	-0.0028	[°/°C]
T₂	-0.0011	-0.0045	6.0e-05	[°/°C]
T_{SRU}	-0.0009	-8.0e-05	-0.0019	[°/°C]
CHU B				
	α	β	γ	
Constant	0.0673	-2.1642	0.4530	[°]
T₁	0.0013	-0.0131	0.0022	[°/°C]
T₂	-0.0006	-0.0036	0.0016	[°/°C]
T_{SRU}	-0.0010	-0.0009	-0.0022	[°/°C]
CHU C				
	α	β	γ	
Constant	-0.0764	2.3342	-0.5756	[°]
T₁	-0.0021	0.0138	-0.0042	[°/°C]
T₂	0.0013	0.0043	-1.0e-05	[°/°C]
T_{SRU}	0.0009	5e-05	-0.0018	[°/°C]
CHU D				
	α	β	γ	
Constant	-0.0374	2.3487	0.4798	[°]
T₁	-0.0017	0.0135	0.0039	[°/°C]

\mathbf{T}_2		0.0013	0.0046	0.0001		[$^{\circ}\text{C}$]
\mathbf{T}_{SRU}		0.0009	0.0008	-0.0017		[$^{\circ}\text{C}$]

209

210 **Table 2: Thermal model coefficients based on PJ 1 (2016-240) for transformation between**
 211 **Juno SC and each of the μASC CHU's.**

212

213 As seen from the model coefficient table, the angular deviation is almost entirely a rotation about
 214 the spacecraft y-axis (β), which is parallel to the solar array hinge line; this is consistent with the
 215 attitude variation observed during cruise (Connerney et al., 2017) in response to the secular
 216 cooling of the array in transit from Earth to Jupiter, during which a rotation of $\sim 1^{\circ}$ of rotation
 217 about spacecraft y axis was observed. It is also the rotation expected of bending due to
 218 unmatched CTE on sunward-facing and dark sides of the solar array.

219

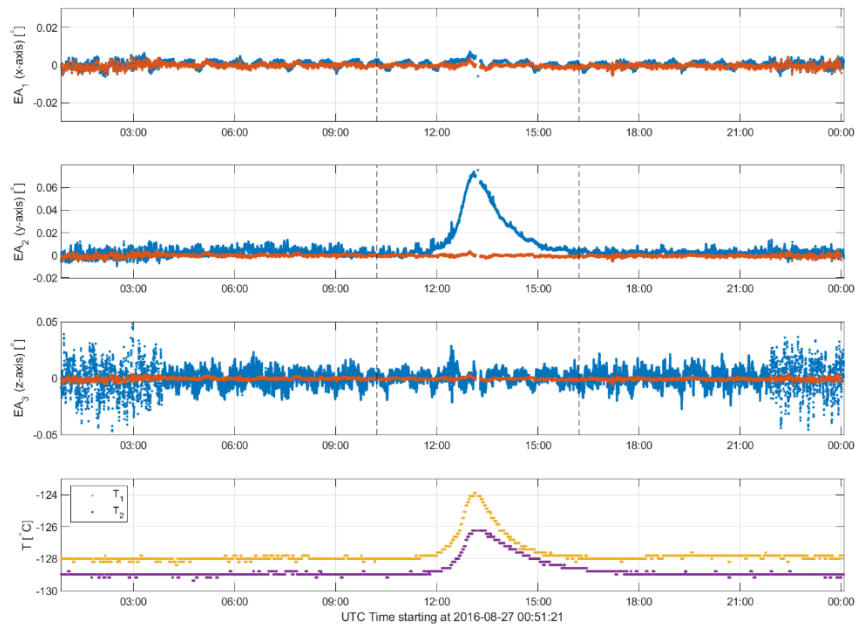
220 3 Results

221 In Figure 6 we show a comparison of the CHU and spacecraft attitudes as measured using a fixed
 222 transformation with that using a variable transformation based on the thermal model output. The
 223 corrected attitudes show significant improvements. The thermal model completely removes the
 224 variation caused by the bending of the boom (rotation about the y axis) and shows virtually no
 225 residual variation apart from white noise. Likewise, the quasi-periodic attitude errors appearing
 226 as rotations about the x and z axis are removed well using the SRU temperature proxy. The root
 227 mean square residual attitude error (RMS) of rotation about the y-axis, after correction, is 8 arc-
 228 seconds, compared to 72.1 arc-seconds found using the uncorrected (static) transformation.

229

230

231



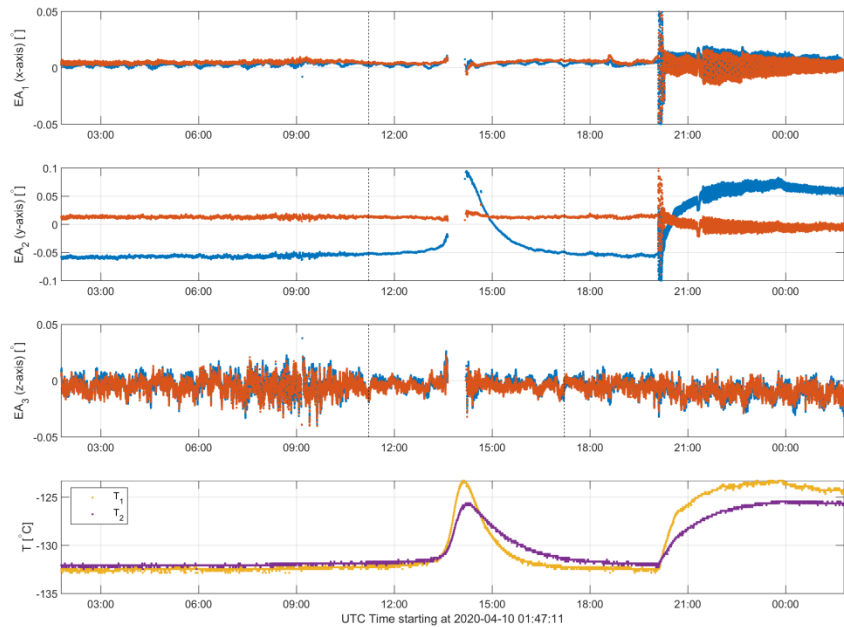
232

233 **Figure 6: Relative comparison of the Juno CHU B and SC orientation in the CHU B**
 234 **reference frame (PJ1, 2016-240). Top three panels: Blue shows uncorrected deflection**
 235 **angles. Red shows deflection angles after correction and applying a 60 seconds moving**
 236 **average. Bottom panel: Shows the two SC solar panel temperatures.**

237

238

239 It is important to mention that modeling was based only on the data from the PJ1 (2016-240).
 240 Application of the model outside of the modeling period (for the PJ3 to PJ27 dataset) shows
 241 similarly good results, as seen in the example illustrated in Fig 7 for periJove 26. By applying the
 242 model to the PJ26 data, RMS of the rotation error about the y-axis is reduced from 129.0 to 8.5
 243 arc-seconds. This is a very impressive result, considering the date we correct for is almost 4
 244 years after the model was computed and that the range of thermal distortion is twice the range of
 245 that used to establish the model parameters.



246

247 **Figure 7: Relative comparison of the Juno CHU B and SC orientation in the CHU B**
 248 **reference frame (PJ26, 2020-101). Top three panels: Blue shows uncorrected deflection**
 249 **angles. Red shows deflection angles after correction and applying a 60 seconds moving**
 250 **average. Bottom panel: Shows the two SC solar panel temperatures.**

251

252 Fig 7 illustrates the model efficacy as applied to an MWR orbit, in which the spacecraft attitude
 253 is altered well in advance of the periJove pass (so that the spacecraft attitude perturbations are
 254 well damped). As a result, the solar array is a bit further off sun as well, and the spacecraft enters
 255 the periJove interval represented here off Earth point, and therefore somewhat cooler than
 256 normal (GRAV orbit). This effect is also well modeled and the corrected attitude is brought back
 257 to nearly 0 degrees for the periJove. The rapid re-orientation about 6 hours post-PJ is somewhat
 258 less well corrected and evidences a long lasting disturbance that slowly yields to the spacecraft
 259 fluid nutation dampers.

260 As demonstrated, the choice of the proxy temperatures and model parameters estimated with the
 261 SVD solution provide excellent compensation of the thermal disturbances. The results after
 262 applying thermal model show virtually no variation of relative orientation between SC and
 263 CHU's, apart from noise and settling effects of the Earth-point precession. Note that modeling
 264 period was based solely on the PJ1 data (2016-240), and the model has been applied on data well
 265 beyond the modelling period and thermal range, up to PJ26. Using the model coefficients, a
 266 NAIF c-kernels is computed for each MOB using a thermo-elastic model (Table 1) of the boom

267 deflection as a function of temperature. These thermo-elastic MOB c-kernels have been provided
268 to NAIF for archive along with the spacecraft c-kernels.

269 Performance of the proposed model for the compensation of Juno wing thermo-elastic instability
270 for periJoves 1-27 can be found in the supplementary material to this paper. Attention to
271 mechanical stability is but one consideration in the measurement accuracy achieved on a flight
272 platform. Juno is the first spacecraft to venture beyond Earth orbit with a magnetic field
273 investigation suitably endowed with sensors to track attitude stability of the magnetometer boom
274 (necessitated by the need to separate spacecraft and magnetic sensors). Juno's very accurate
275 vector magnetic field measurements also revealed the presence of relatively small spacecraft
276 fields generated within the conductive MAG boom structure itself as the spacecraft slowly spins
277 (2 rpm) in the presence of a strong magnetic field (Eddy current generation). Correction for this
278 effect was described by Kotsiaros et al. (2020) who presented a finite element model of Eddy
279 current generation in the vicinity of the MAG sensors. This effort and the thermal modeling
280 described here illustrate the need for a comprehensive systems approach in achieving high
281 accuracy measurements on space platforms.

282

283 **Acknowledgements:** We thank the project and support staff at the Jet Propulsion Laboratory (JPL),
284 Lockheed Martin, and the Southwest Research Institute (SWRI) for the design, implementation, and
285 operation of the Juno spacecraft. We are particularly indebted to Lockheed Martin mechanical
286 engineer, Russ Gehring, who was responsible for the design and fabrication of the MAG boom.
287 JPL manages the Juno mission for the principal Investigator, S. Bolton, of SWRI. This research is
288 supported by the Juno Project under NASA grant NNM06AAa75c to SWRI, and NASA grant
289 NNN12AA01C to JPL/Caltech. The Juno mission is part of the New Frontiers Program managed at
290 NASA's Marshall Space Flight Center in Huntsville, Alabama. The authors are aware of no real or
291 perceived conflicts of interest with respect to the results of this paper. All data used in this article is
292 available in the main text and in the supplementary materials, as well as in the permanent archival data
293 repository, Zenodo (Herceg et al, 2020).

294

295 **References**

296 Bolton, S.J., Lunine, J., Stevenson, D. *et al.* The Juno Mission. *Space Sci Rev* **213**, 5–37 (2017).
297 <https://doi.org/10.1007/s11214-017-0429-6>

298 Connerney, J.E.P., Benn, M., Bjarno, J.B. *et al.* The Juno Magnetic Field Investigation. *Space*
299 *Sci Rev* **213**, 39–138 (2017). <https://doi.org/10.1007/s11214-017-0334-z>

300 Connerney, J.E.P., Lawton, P., Kotsiaros, S., Herceg, M. The Juno Magnetometer (MAG)
301 Standard Product Data Record and Archive Volume Software Interface Specification (SIS)

302 Herceg, M., Jørgensen, P.S., Jørgensen, J. L. Characterization and compensation of thermo-
303 elastic instability of SWARM optical bench on micro Advanced Stellar Compass attitude
304 observations, *Acta Astronautica*, Volume 137, August 2017, Pages 205-213.
305 <https://doi.org/10.1016/j.actaastro.2017.04.018>

306 Kotsiaros, S., Connerney, J. E. P., and Martos, Y. (2020). Analysis of Eddy current generation on
307 the Juno spacecraft in Jupiter's magnetosphere, *Earth and Space Science*,
308 doi:10.1029/2019EA001061

309 Herceg, M., Jørgensen, P.S., Jørgensen, J. L., J.E. Connerney: Supplementary material for *Thermo-*
310 *elastic response of the Juno spacecraft's solar array/magnetometer boom*, Zenodo DOI:
311 10.5281/zenodo.3936080

312

313

314